

****FULL TITLE****

*ASP Conference Series, Vol. **VOLUME**, **YEAR OF PUBLICATION***

****NAMES OF EDITORS****

The New Solar Telescope in Big Bear: Polarimetry II

W. Cao, K. Ahn, P. R. Goode, S. Shumko, N. Gorceix and R. Coulter

*New Jersey Institute of Technology, Center for Solar-Terrestrial
Research, 323 Martin Luther King Blvd., Newark, NJ 07102, USA*

*Big Bear Solar Observatory, 40386 North Shore Lane, Big Bear City,
CA 92314, USA*

Abstract. IRIM (Infrared Imaging Magnetograph) is one of the first imaging solar spectro-polarimeters working in the near infrared (NIR). IRIM is being installed and commissioned in the Coudé Lab of the 1.6-meter New Solar Telescope (NST) at Big Bear Solar Observatory (BBSO). This innovative system, which includes a 2.5 nm interference filter, a unique 0.25 nm birefringent Lyot filter, and a Fabry-Pérot etalon, is capable of providing a bandpass as low as 0.01 nm over a field-of-view of $50''$ in a telecentric configuration. An NIR waveplate rotates ahead of M3 in the NST as the polarimeter modulator, and ahead of it locates a calibration unit to reduce polarization cross-talk induced by subsequent oblique mirrors. Dual-beam differential polarimetry is employed to minimize seeing-induced spurious polarization. Based on the unique advantages in IR window, the very capable NST with adaptive optics, IRIM will provide unprecedented solar spectro-polarimetry with high Zeeman sensitivity ($10^{-3}I_c$), high spatial resolution ($0.2''$), and high cadence (15 s). In this paper, we discuss the design, fabrication, and calibration of IRIM, as well as the results of the first light observations.

1. Introduction

The largest aperture solar telescope, the 1.6-m clear aperture New Solar Telescope (NST) has been installed and is being commissioned at Big Bear Solar Observatory (BBSO). The NST (Goode et al. 2010a) has an off-axis Gregorian configuration with a focal ratio of $f/52$, and is equipped with facility-class post-facto instruments for high resolution solar photometry, spectrometry, and polarimetry spanning the visible to the near infrared (NIR). The currently planned post-facto instruments (Cao et al. 2010a) include the Nasmyth Focus Filtergraphs (Cao et al. 2010b), the Cryogenic Infrared Spectrograph (CYRA), Adaptive Optics (AO-76, AO-308), the Infrared Imaging Magnetograph (IRIM), the Visible Imaging Magnetograph (VIM), and the Fast Imaging Solar Spectrograph (FISS). As of now, the Nasmyth Focus Filtergraphs have been installed for the NST commissioning and first light photometry observations have been made. Diffraction limited images were there obtained frequently after processed using a post-facto speckle reconstruction algorithm. The first generation adaptive optics for the NST, AO-76, has been successfully developed and provides turbulence correction for all instruments in the Coudé Lab. Meanwhile, FISS has been put into routine operation to offer fast imaging spectrometry in Ha 656 nm and Ca II 854 nm, simultaneously.

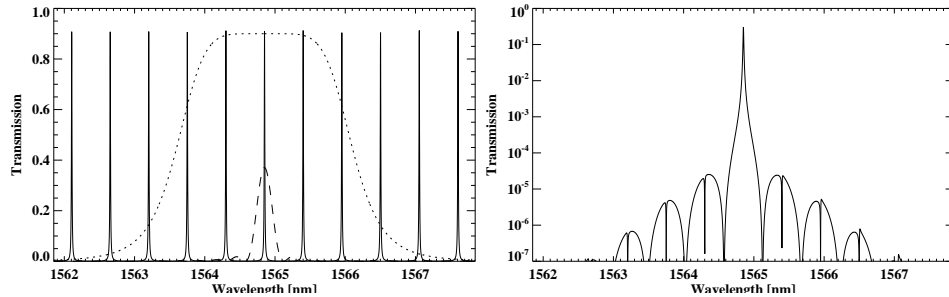


Figure 1. *Left:* Transmission profiles of the FPI (solid curve), the Lyot filter (dashed curve), and the interference filter (dotted curve). *Right:* Transmission profile of the IRIM.

IRIM is the first available polarimetric instrument of the NST. Benefitting from a number of observational advantages in the NIR, such as sufficient Zeeman splitting, weak instrumental polarization, low stray light, as well as better seeing conditions, IRIM probes the magnetic fields in the deepest layer of the photosphere with a Zeeman sensitive line pair: Fe I 1564.85 nm ($g_{eff} = 3$) and Fe I 1565.29 nm ($g_{eff} = 1.53$). In contrast to spectrograph-based polarimeters that are currently operational in the NIR, IRIM is the first imaging magnetograph based on Fabry-Pérot Interferometer (FPI) working in the NIR, which offers 2-D spectro-polarimetry data over its field-of-view (FOV) of $50''$. With the aid of the large aperture and over 2 m^2 photon collecting area of the NST, as well as AO system, IRIM will provide spectro-polarimetry of vector fields with high Zeeman sensitivity ($10^{-3} I_c$), diffraction limited resolution ($0.2''$), and high cadence (15 s).

2. Optical Design

IRIM is designed to have a moderate spectral resolving power of $> 10^5$ and a low parasitic contamination level of $< 10^{-4}$. To achieve this goal, a 70 mm aperture FPI is combined with a Lyot filter with a FWHM of 0.25 nm and an interference filter (FWHM $\sim 2.5 \text{ nm}$) to provide a bandpass of $\sim 0.1 \text{ \AA}$ in a telecentric optical configuration. Figure 1 shows the transmission profiles of each component and the whole system. Due to the low transmission of the Lyot filter, the throughput is only 30% for incoming polarized light.

FOV always competes with maximum $f^\#$ in keeping Lagrange optical invariance. In a telecentric configuration, a large incident angle of a beam (or small $f^\#$) on the FPI causes a broadening of its effective bandpass. Compromising between the effective bandpass and limited space in the Coudé lab, the final $f^\#$ for the FPI is determined to have a $f^\#$ of 125. Therefore, the FOV has a square size of $50''$ by $50''$. Four doublet lenses are employed to comprise the optical path in a diffraction limited configuration. Figure 2 sketches the schematic layout of the IRIM main optical path.

The polarimeter of IRIM consists a modulator, a analyzer and a calibration unit, which has been described in detail by Goode, et al. (2010b). The

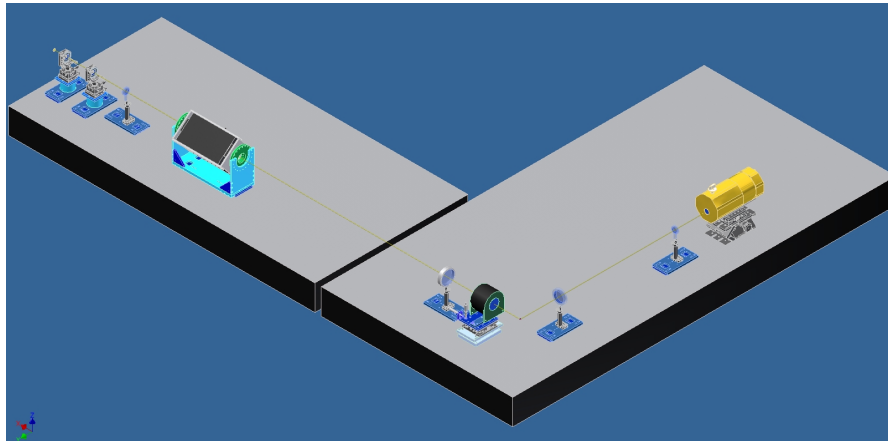


Figure 2. Schematic layout of the IRIM main optical path. Along the light beam from left to right are two Wollaston prisms, doublet 1, Lyot filter, doublet 2, FPI, doublet 3 and 4, and NIR camera. Auxiliary and calibration optical paths are not shown here.

modulator is a zero-order waveplate with a retardation of $0.3525\lambda \pm \lambda/350$ at 1564.85 nm. It was fabricated by sandwiching a birefringent polymer between a pair of BK7 grade A fine annealed glass. The waveplate has a 5.5 inch aperture with a wavefront distortion of $\leq \lambda/4$, accommodating the large beam size ahead of M3. Beam deviation was reduced to less than 2 arc min so AO-76 is able to correct the beam wobbling while rotating. To minimize seeing-induced spurious polarization, two Wollaston prisms are adopted as the analyzers to offer a dual-beam for differential polarimetry. The first one acts as a polarizing beam splitter, while the second makes the beam parallel. The Wollaston prism is a combination of two calcite sheets, each having its fast axis orthogonal to the other. The surface between the two sheets is wedged by 5° . Though two Wollaston prisms introduce some aberration, no corrective optics are added since the aberration is within the diffraction limit on the detector in the NIR. Due to the existence of linear polarizers inside the Lyot filter, the Wollaston prisms are placed in front of it. Meanwhile, the optical axis of the Lyot filter has to be orientated at 45° with respect to that of the Wollaston prisms to allow the same light throughput for dual-beam differential polarimetry.

3. Implementation and Calibration

In comparison with instruments working in the visible, the implementation and calibration of IRIM are more challenging since the infrared can't be sensed by either the human eye or a common Si-CCD camera. The detailed calibration procedures of IRIM and its sub-systems, such as the FPI, Lyot filter, and NIR camera have been discussed in previous papers (Cao et al., 2004, 2006a, 2006b, 2010c). The calibration and operation of IRIM polarimeter follow the

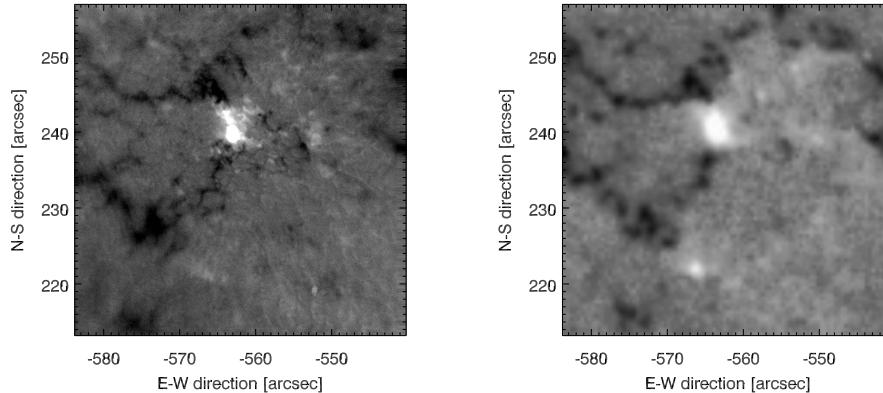


Figure 3. A comparison of line-of-sight magnetogram taken with IRIM (*left*) and SDO (*right*) on September 23 2010.

approach and procedures in Elmore (2001, private communication) and Goode et al. (2010b).

IRIM offers four operating modes: spectrometry mode, polarimetry mode, Doppler mode and photometry mode. A typical spectrometry observation involves scanning over the spectral line with 25~30 wavelength points. The line profiles can be derived from the same features (corresponding to a single pixel or a cluster of pixels) after image processing: alignment, destretching and deconvolution. The cadence of spectrometry mode is about 5 s. The polarimetry is the most complicated observational mode. Much effort have been made to improve the cadence and synchronization between rotating waveplate and image acquisition by camera. Limited by available NIR photons, the rotating rate is set up at 1 revolution/s only. The camera works in a free-run mode at a frame rate of 16 frame/s. In one revolution, the IRIM control computer transfers data of 1st-16th frames from the framegrabber to the computer memory. Meanwhile, it commands the FPI to shift wavelength to the next scanning point. These two tasks have to be completed within one frames timing. Therefore, the 17th frame must be discarded. From the 18th frame, the next burst begins for another 16 frames. This procedure is repeated until it finishes all spectral tuning with, typically, 11 wavelength points. So, the spectro-polarimetry cadence is around 15 s. After a series of post-processing including dark and flat field corrections, rectifying spectra, removal of the instrument profile, and polarimetric calibration, etc., the IRIM polarimetry data are the input to the Stokes inversion code for inferring maps of vector field strengths.

4. First Light Magnetogram

IRIM is being commissioned in the Coudé Lab of the NST at BBSO. Figure 3 shows the capability of IRIM at high spatial resolution. The left panel shows a line of sight magnetogram taken with IRIM on 2010 September 23. This image is a combination of 25 frames for each polarization state under fair seeing conditions. Due to seeing, AO-76 only could work inside an isoplanatic patch of

about $20'' \times 20''$. The right panel is a cropped image of a SDO/HMI magnetogram with the same FOV as the IRIM image, and with a time difference of 6 mins. It is clear that IRIM shows outstanding results with the shown high resolution magnetogram.

We gratefully acknowledge the support of NSF (AGS-0847126 and AGS-0745744), NASA (NNX08BA22G) and AFOSR (FA9550-09-1-0655).

References

- Cao, W., Gorceix, N., Coulter, R., Ahn, K., Rimmele, T. R., & Goode, P. R. 2010a, *Astron. Nachr.*, 331, 636
- Cao, W., Gorceix, N., Coulter, R., Wöger, F., Ahn, A., Shumko, S., Varsik, J., Coulter, A., & Goode, P. R. 2010b, *SPIE*, 7735, 77355V
- Cao, W., Coulter, R., Gorceix, N., & Goode, P. R. 2010c, *SPIE*, 7742, 774220
- Cao, W., Jing, J., Ma, J., Xu, Y., Wang, H., & Goode, P. R. 2006a, *PASP*, 118, 838
- Cao, W., Hartkorn, K., Ma, J., Xu, Y., Spirock, T., Wang, H., & Goode, P. R. 2006b, *Solar Phys.*, 238, 207
- Cao, W., Denker, C., Wang, H., Ma, J., Qu, M., Wang, J., & Goode, P. R. 2004, *SPIE*, 5171, 307
- Elmore, D. 2001, CPA Theory of Operation
- Goode, P. R., Coulter, R., Gorceix, N., Yurchyshyn, V., & Cao, W. 2010a, *Astron. Nachr.*, 331, 620
- Goode, P. R., Cao, W., Ahn, K., Gorceix, N., & Coulter, R. 2010b, in this proceeding